

# Switching of magnetic domains reveals spatially inhomogeneous superconductivity

Simon Gerber, Marek Bartkowiak, Jorge L. Gavilano, Eric Ressouche, Nikola Egetenmeyer, Christof Niedermayer, Andrea D. Bianchi, Roman Movshovich, Eric D. Bauer, Joe D. Thompson and Michel Kenzelmann

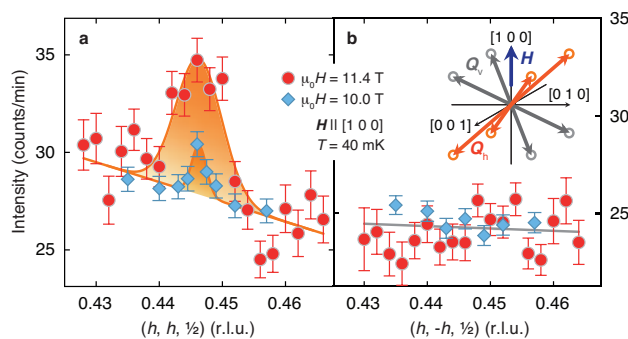
## Supplementary discussion: Spin-density wave domains in the $Q$ -phase

We briefly explain the  $Q$ -phase state in terms of SDW domains. A real space representation of the two possible SDW structures is shown in figure 2a and 2b. Both the  $Q_h$ - (orange) and the  $Q_v$ -domain (grey) have modulated magnetic moments  $\mathbf{M} \parallel [0\ 0\ 1]$ , but propagate in orthogonal directions (arrows). In reciprocal space, the two domains are described by two subsets of  $Q$ -vectors forming an eightfold star of  $Q$ -vectors as schematically depicted in figure 2c of the main article. By mirror and translational symmetry, the eight  $Q$ -vectors can be attributed to either the horizontal  $\mathbf{Q}_h = (q, q, 0.5)$  or the vertical  $\mathbf{Q}_v = (q, -q, 0.5)$  wave vector as shown in orange and grey, respectively. However, the two domains are not equivalent in the depicted geometry with  $\mathbf{H} \parallel [1\ -1\ 0]$ :  $\mathbf{Q}_v$  has components parallel to  $\mathbf{H}$  and  $\mathbf{Q}_h$  only perpendicular components. For  $\mathbf{H} \parallel [1\ 0\ 0]$ , the two domains are degenerate with equal components parallel to the field direction (see sketch in Fig. S1b).

A  $q$ -scan along  $[1\ -1\ 0]$  around  $(0.44, 0.44, 0.5)$  at  $\mu_0 H = 11.2$  T confirms long-range magnetic order along  $\mathbf{H} \parallel [1\ -1\ 0]$ , with a lower bound of the vertical correlation length of 300 Å. Three-dimensional long-range SDW order was found earlier<sup>31</sup> also for  $\mathbf{H} \parallel [1\ 0\ 0]$ .

## Supplementary discussion: Single- $Q$ spin-density wave order for $\mathbf{H} \parallel [1\ 0\ 0]$

Only one SDW domain was examined for the determination of the magnetic structure of the  $Q$ -phase in the earlier study<sup>31</sup> with  $\mathbf{H} \parallel [1\ 0\ 0]$ . Since this field direction does not break the symmetry equivalence of the two magnetic domains (see sketch in Fig. S1b), it was expected that both magnetic domains are present. On the diffractometer D23 we revisited this case: 18 nuclear reflections were used in the alignment and a precision of  $0.06^\circ$  and  $0.15^\circ$  with respect to the magnetic field direction was obtained in the direction of  $[0\ 1\ 0]$  and



Supplementary Figure 1. **Mono-domain single- $Q$  magnetism for  $H \parallel [1 0 0]$ .** The two spin-density wave domains are degenerate with respect to the field direction, the crystal structure and the  $d_{x^2-y^2}$ -wave gap function when  $H \parallel [1 0 0]$  (see sketch in **b**). Within the accuracy of the alignment, a mono-domain population is found as well: magnetic Bragg peaks appear only at  $Q_h$ - (**a**) but not at  $Q_v$ -positions (**b**). Single- $Q$ , long-range ordered magnetism is also observed close to the lower  $Q$ -phase boundary ( $\mu_0 H = 10.0$  T, blue diamonds). Scans are shown in reciprocal lattice units (r.l.u.). Lines depict Gaussian fits to the data with a common background for the  $\mu_0 H = 10.0$  and 11.4 T data. Error bars, 1. standard deviation.

$[0 0 1]$ , respectively. It is important to note that only a misalignment along  $[0 1 0]$  affects the degeneracy of the SDW domains as a result of the commensurability along  $[0 0 1]$ . We probed the domain population in this geometry by searching for magnetic scattering at the top four positions of the eightfold star of  $Q$ -vectors.

Data presented in figure S1a and S1b show the surprising experimental result, that for  $H \parallel [1 0 0]$  only the  $Q_h$ -domain is populated, but not the  $Q_v$ -domain. Preparing the magnetic state at  $\mu_0 H = 11.4$  T and  $T = 50$  mK by ramping  $H$  from below the lower  $Q$ -phase boundary or by quenching through the first-order superconducting transition did not result in a different domain population. In view of the precise sample alignment this points to a hypersensitivity of the domain population with respect to the magnetic field direction.

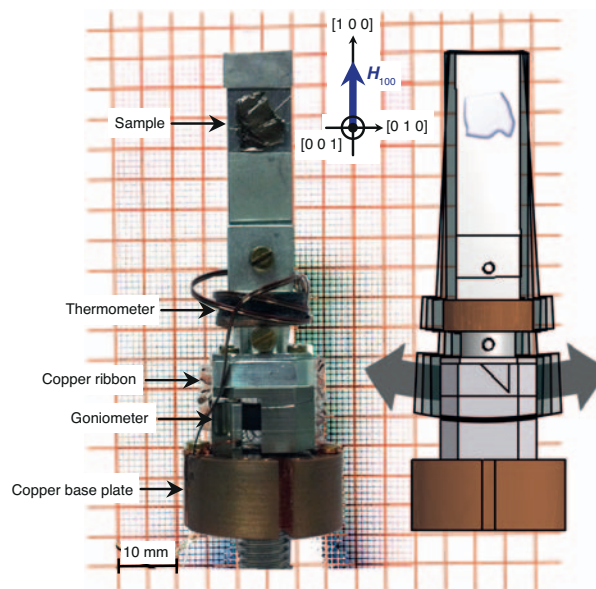
We take advantage of the mono-domain population, described by a single  $Q$ -vector, to test whether a double- $Q$  state is realised at the lower  $Q$ -phase boundary as theoretically suggested<sup>32,33</sup>. A double- $Q$  structure is described by coherent superposition of a  $Q_v$ - and  $Q_h$ -modulation, and thus magnetic scattering at both kinds of magnetic Bragg positions should be observed in the experiment. Double- $Q$  antiferromagnetism could, in principle,

also account for the nuclear magnetic resonance (NMR) line broadening<sup>34</sup> observed in this field range. Data, represented by blue diamonds in figure S1a and S1b, were measured at  $\mu_0 H = 10.0$  T, i.e., in the field-range, where NMR data may be explained by a double- $Q$  structure. Our data shows a single- $Q$  SDW mono-domain at this field strength as well, which excludes the presence of an additional double- $Q$ -phase in the examined field range.

### Supplementary methods: **Piezoelectric *attocube* sample rotator**

Measurements described in the previous section imply that the switching between the two possible SDW domains happens in a very narrow range around  $\mathbf{H} \parallel [1\ 0\ 0]$ . To reach the alignment precision needed, we devised a sample rotator which operates at low temperatures and high magnetic fields. Our setup is based on a purpose-built non-magnetic piezoelectric goniometer (type *ANGt50* from *attocube systems AG*), providing an angular range  $\Delta\psi = \pm 3.6^\circ$  and requiring a sample space diameter of only 20 mm—small enough to fit the 31 mm diameter available inside the *Kelvinox-VT* dilution refrigerator. A Copper base plate was used to fix the goniometer. The pre-aligned sample was glued to a 0.5 mm thick pure Aluminium plate and mounted at the top of the goniometer together with a Ruthenium oxide thermometer (see Fig. S2). The goniometer body is made from Titanium and the rotor as well as the stator are mechanically only coupled via the piezo crystal. Two corrugated Copper ribbons were spanned between the base plate and the rotor of the goniometer to provide proper thermal contact between the sample and the dilution refrigerator. The ribbon was made from a 12  $\mu\text{m}$  thick, 6 mm wide and 22 mm long pure Copper foil (99.99+). By choosing a foil for the coupling rather than a wire, the cross section corresponds to a wire of 420  $\mu\text{m}$  diameter, we ensure both good mechanical flexibility and good thermal conductivity. The whole setup was preassembled and the base plate was fixed to the copper rod extending from the mixing chamber of the dilution refrigerator towards the centre of the magnet, e.g., the neutron beam.

A base temperature of  $T_s = T_{\text{mix}} = 38$  mK was reached at zero magnetic field, whilst we obtained a sample temperature of  $T_s = 65$  mK at  $\mu_0 H = 11.4$  T ( $T_{\text{mix}} = 40$  mK at the mixing chamber). The elevated sample temperature in high magnetic fields can be explained by the additional heat input due to eddy currents and the reduction of the thermal conductivity of Copper. Moreover, the increased specific heat of the assembly at high magnetic fields raised



Supplementary Figure 2. **Piezoelectric attocube sample rotator.** The goniometer is fixed to a Copper base plate and thermally linked to the mixing chamber of the dilution refrigerator. A sample platform is mounted on the moving part of the goniometer, which consists of an Aluminium base plate for the Ruthenium oxide thermometer, a Hall sensor and the sample holder. The single-crystalline  $\text{CeCoIn}_5$  sample is glued to a 0.5 mm thick pure Aluminium plate. Thermal anchoring of the sample assembly to the Copper base plate is achieved by two corrugated Copper ribbons.

the equilibration times from about 10 minutes to over 1 hour.

The most dominant source of heat is the goniometer drive. Any movement of the goniometer introduces heat into the system, since a piezo-motor works on the principle of slip-stick friction. We operated the piezo-drive with an input voltage of 30 V and a repetition rate of 100 Hz. A full sweep took about 10 minutes and heated the sample to above  $T_s = 6$  K while the mixing chamber reached  $T_{\text{mix}} = 1.2$  K. Typical moving angles in the experiment were of the order of  $\Delta\psi = 0.5\text{-}1.0^\circ$ . It was not possible to precisely determine the angle of rotation  $\psi$  from the step count due to the working principle of the goniometer. However, using the neutron diffractometer during the thermalisation of the sample allowed for a quantification of better than  $\Delta\psi = 0.01^\circ$  via the vertical tilt of  $(0, k, l)$  nuclear Bragg peaks.

In order to test the functionality of the setup prior to the neutron scattering experiment, we attached a miniature Hall sensor (type *HS-80* from *Advanced Hall Sensors Ltd.*) to

the sample platform. This allowed us to use the magnetic field of the cryomagnet or even the stray field of a permanent magnet, fixed to the outside of the cryostat, to monitor the sample rotation.

### Supplementary methods: **Preparation of the $Q$ -phase state**

The strong heat load during rotation of the piezo-electric *attocube* sample rotator caused the sample temperature to raise above the superconducting transition temperature, thereby destroying the  $Q$ -phase state. We exploited this fact to rule out any history-dependent effects that might influence the domain switching shown in figure 3a. First, we moved the goniometer and raised the sample temperature above  $T_s = 1.5$  K. We utilised the sample thermometer as a heater, whenever the goniometer did not generate sufficient heating. Then, we realigned the single-crystal and determined the angle of rotation  $\psi$  (see Fig. 3b). With the sample still in the normal state we lowered the magnetic field from  $\mu_0 H = 11.4$  T to 9.0 T. Then, we waited until the superconducting state was entered through the second-order phase transition and a sample temperature of  $T_s = 100$  mK was reached. At this point, the sample is in the non-magnetic main  $d$ -wave superconducting state, but not yet in the  $Q$ -phase state (see inset of Fig. 1b). Finally, the  $Q$ -phase was entered through another second-order phase transition at  $\mu_0 H_Q \approx 9.8$  T by ramping the magnetic field from  $\mu_0 H = 9.0$  T to 11.4 T, while keeping the temperature around  $T_s = 100$  mK.

To measure the hysteresis of the domain switching (see Fig. 3c and 3d) we had to be very careful not to destroy the  $Q$ -phase state by heating during movement of the goniometer. The piezo was driven for only about 3 sec, which corresponds to a rotation angle of about  $\Delta\psi = 0.04^\circ$  and caused a temperature increase at the sample of less than 20 mK. In order to assure reproducible measurement conditions, the sample was then allowed to cool to  $T_s = 100$  mK, which took about 15 minutes.

---

<sup>31</sup> Kenzelmann, M. *et al.* Evidence for a magnetically driven superconducting  $Q$  phase of CeCoIn<sub>5</sub>. *Phys. Rev. Lett.* **104**, 127001 (2010).

<sup>32</sup> Kato, Y., Batista, C. D. & Vekhter, I. Antiferromagnetic order in Pauli-limited unconventional

superconductors. *Phys. Rev. Lett.* **107**, 096401 (2011).

<sup>33</sup> Kato, Y., Batista, C. D. & Vekhter, I. Structure of magnetic order in Pauli limited unconventional superconductors. *Phys. Rev. B* **86**, 174517 (2012).

<sup>34</sup> Koutroulakis, G. *et al.* Field evolution of coexisting superconducting and magnetic orders in CeCoIn<sub>5</sub>. *Phys. Rev. Lett.* **104**, 087001 (2010).